Sea-ice eukaryotes of the Gulf of Finland, Baltic Sea, and evidence for herbivory on weakly shade-adapted ice algae

Markus Majaneva*[a,b,c,1], Jaanika Blomster[b], Susann Müller[a,b], Riitta Autio[c], Sanna Majaneva[a,b,c], Kirsi Hyytiäinen[a,b], Satoshi Nagai[d], Janne-Markus Rintala[a,b,c]

[a]Tvärminne Zoological Station, University of Helsinki, J.A. Palménin tie 260, 10900 Hanko, Finland

[b]Department of Environmental Sciences, University of Helsinki, P.O. Box 65, 00014 Helsinki, Finland

[c]Marine Research Centre, Finnish Environment Institute, P.O. Box 140, 00251 Helsinki, Finland

[d]Research Center for Aquatic Genomics, National Research Institute of Fisheries Science, Kanazawa-ku 236-8648, Japan

*Corresponding author, e-mail: markus.majaneva@gmail.com

[1]Present address: Department of Natural History, NTNU University Museum, Norwegian University of Science and Technology, Trondheim, Norway and Linnaeus University Centre for Ecology and Evolution in Microbial Model Systems, Kalmar, Sweden

Abstract

To determine community composition and physiological status of early spring sea-ice organisms, we collected sea-ice, slush and under-ice water samples from the Baltic Sea. We combined light microscopy, HPLC pigment analysis and pyrosequencing, and related the biomass and physiological status of sea-ice algae with the protistan community composition in a new way in the area. In terms of biomass, centric diatoms including a distinct *Melosira arctica* bloom in the upper intermediate section of the fast ice, dinoflagellates, euglenoids and the cyanobacterium *Aphanizomenon* sp. predominated in the sea-ice sections and unidentified flagellates in the slush. Based on pigment analyses, the ice-algal communities showed no adjusted photosynthetic pigment pools throughout the sea ice, and the bottom-ice communities were not shade-adapted. The sea ice included more characteristic phototrophic taxa (49%) than did slush (18%) and under-ice water (37%). Cercozoans and ciliates were the richest taxon groups, and the differences among the communities arose mainly from the various phagotrophic protistan taxa inhabiting the communities. The presence of pheophytin *a* coincided with an elevated ciliate biomass and read abundance in the drift ice and with a high *Eurytemora affinis* read abundance in the pack ice, indicating that ciliates and *Eurytemora affinis* were grazing on algae.

Keywords

18S rRNA gene; Accessory pigments; Herbivory; Photoacclimation; Sea ice

Introduction

Sea ice is composed of solid ice and saline water called brine (Petrich and Eicken 2010). Brine lies and flows in pockets and interconnected channels within the sea ice, offering habitats for small-sized organisms. The diameter of the brine pockets and channels varies from 1 µm to several centimetres (Eicken et al. 1995), depending on the temperature and salinity of the parent water (Palosuo 1961; Petrich and Eicken 2010). The habitable space within the ice is substantially smaller at the low temperatures (< -10 °C) occurring during winter than at the near-zero temperatures of spring. In addition, the volume of the brine-channel system is considerably reduced in low-salinity seas such as the Baltic Sea (salinity range 3–10), compared with truly marine seas (salinity > 24). Due to the small size of the brine channels, the Baltic eukaryotic community consists mainly of protists, and the only notable metazoans present are rotifers and copepod nauplii (Kaartokallio 2004; Meiners et al. 2002; Norrman and Andersson 1994).

Knowledge of the taxonomy and ecology of Baltic Sea ice-algal communities has accumulated since the first studies were conducted (Hällfors and Niemi 1974; Häyrén 1929; Hickel 1969; Huttunen and Niemi 1986; Niemi 1973), and it has been estimated that these algal communities contribute about 10% of the primary production during the ice-covered season (Haecky and Andersson 1999). Usually, the predominant autotrophic eukaryotes are diatoms (Haecky et al. 1998; Meiners et al. 2002; Norrman and Andersson 1994), but in contrast to Arctic sea ice, the dinoflagellate and green algal biomass is considerable in Baltic Sea ice (Kaartokallio et al. 2007; Piiparinen et al. 2010; Rintala et al. 2010). Another peculiarity of Baltic Sea ice is that the surface-layer algal biomass may significantly contribute to the overall algal biomass (Meiners et al. 2002; Piiparinen and Kuosa 2011; Piiparinen et al. 2010).

The heterotrophic compartment of the eukaryotic community in Baltic Sea ice is less well known; previous studies have not included detailed identification of heterotrophic protists, with the exception of publications by Vørs (1992), Ikävalko and Thomsen (1996; 1997) and Ikävalko

(1998). The lack of detailed species identification is not due to indolence on the part of these early investigators, but rather that many species cannot be identified with light microscopy (LM) (e.g. Lowe et al. 2011). The same issue also holds for the smaller (< 10 µm) autotrophic flagellated eukaryotes. These challenges to identification may be disentangled, using elaborate electron microscopy techniques (e.g. Vørs 1992), but also more indirectly by analysing pigments, using high-performance liquid chromatography (HPLC) (Bidigare et al. 2005) or more cost-effectively and thoroughly by molecular methods (Logares et al. 2012).

Pigment analyses have been routinely used in phytoplankton research (Jeffrey et al. 2011) and to some extent in sea-ice research (Alou-Font et al. 2013; Kudoh et al. 2003), but not yet in research on Baltic Sea ice algae. Identifying algal taxa based on pigment data is not straightforward, since many pigments are found in several algal groups (e.g. fucoxanthin in diatoms, haptophytes and chrysophytes), and at the very best, taxa can be identified to genus level (Zapata et al. 2004) but usually to class level (Jeffrey et al. 2011). In addition, the downward-attenuating light conditions in the sea-ice column strongly affect cellular pigment composition (Alou-Font et al. 2013) and algae acclimate to changing light climates by adjusting their pigment pool. In the case of light-harvesting chlorophylls and carotenoids, this regulation occurs on a time scale of hours, and in photoprotective xanthophyll-cycle pigments from 1 to several hours (Claustre et al. 1994; Moline 1998). Hence, the ratios of various accessory pigments to chlorophyll *a* (chl-*a*) and photosynthetic carotenoids (PSCs) to photoprotective carotenoids (PPCs) are widely used indicators of photoacclimation in algae (e.g. Alou-Font et al. 2013; Arrigo et al. 2014). In addition, during the senescence and death of the cells, the chl-*a* synthesized by algae undergoes degradation to a variety of chl-*a* derivatives, e.g. pheophytin *a*, and thus the presence of pheophytin *a* can be used as an indicator of cell senescence and grazing (Louda et al. 1998; Prins et al. 1991; Strom 1993).

DNA-based approaches have proven to be useful, e.g. for detecting ciliates and flagellates that are difficult to distinguish under LM, and have revealed that heterotrophic protistan taxon richness is higher in sea ice than observed by microscopy (Comeau et al. 2013; Majaneva et al. 2012). As in pigment analysis, DNA sequencing has its own limitations; e.g. taxa are not identified to species level, but the 18S ribosomal RNA (rRNA) gene is used as a proxy for species. The level to which individual taxa can be identified is variable and may be restrained by imperfect reference databases and lineage-specific evolutionary rates in the 18S rRNA gene (Caron et al. 2009). The number of 18S rRNA gene copies per cell also varies from one to tens of thousands among different eukaryotes (e.g. Zhu et al. 2005), resulting in values that represent not the cellular abundance but the number of 18S rRNA gene copies in the sample. At the same time, no other method can identify all eukaryotic micro-organisms, including cryptic species (Lowe et al. 2011), with the same precision and efficiency as sequencing. Consequently, molecular methods are sovereign tools in differentiating protistan communities (e.g. Comeau et al. 2013).

Here, our aim was to relate the biomass and physiological status of sea-ice algae to the protistan community composition in the Gulf of Finland, Baltic Sea. First, we determined the pigment composition of the sea-ice samples, using HPLC to measure the response of the algae to downward-attenuating light conditions. Secondly, we enumerated the dominant taxa and their biomass, using LM. Thirdly, we pyrosequenced the partial 18S rRNA genes of eukaryotes to identify the eukaryotic taxa present in the samples.

Material and Methods

Sampling

We collected 20 samples (15 sea-ice, 3 slush and 2 under-ice water samples) from three research vessel (R/V) Aranda sea-ice cruise stations (Gulf of Finland, Baltic Sea, 8–19 March, 2010): a drift-ice station on 9 March (59°55.67' 26° 01.08'), a heavily packed fast-ice station on 11 March (60°14.30' 26°37.56') and a level fast-ice station on 13 March (60°19.66' 26°51.73'; Supplementary figure 1).

We collected the ice samples with a motorized Cold Regions Research and Engineering Laboratory (CRREL)-type ice-coring auger (9 cm internal diameter, Kovacs Enterprises LLC, Roseburg, OR, USA). We obtained seven ice cores from each station: one for temperature measurements, one for ice structure and five for all the remaining measurements. The five cores were immediately sectioned into five pieces of approximately equal size: surface, upper intermediate, middle, lower intermediate and bottom sections. Thus, the sections varied in size, depending on the ice thickness of each core (43–112 cm). At each location, we placed all five surface sections into a plastic bag, all five bottom sections into another plastic bag, and so on. The ice was then crushed inside the bags, transferred to a bucket and left to melt in darkness at +4° C without filtered seawater, as shown in Rintala et al. (2014). We took three replicate slush samples at the fast-ice station, each replicate 2 m apart. We shovelled each replicate from an approximately 50-cm x 50-cm square and left them to melt in a basket in darkness at +4 °C. We sampled the under-ice water by submersing 1-l bottles in the corer holes at the drift-ice and fast-ice stations.

Ice physics

We measured the ice temperatures at 5-cm intervals immediately after sampling, and we used the bulk salinities of the melted ice samples for calculating the brine volume (%) estimates (Cox and Weeks 1983; Leppäranta and Manninen 1988). We sealed the ice-structure cores in a plastic bag and stored them frozen until the crystal structure was analysed. For the analyses, the ice cores were split lengthwise and cut into 10–20-cm-long and 1-cm-thick ice sections. These ice sections were

frozen on glass plates and planed to thin sections of about 1 mm (Sinha 1977). The thin sections were placed in polarized light between two crossed polarization plates and classified as columnar, transitional or snow ice, based on crystal size and shape. All the work was carried out at -20°C.

Nutrients

The concentrations of inorganic (NO_3 + NO_2, NO_2) and total (tot-N) nitrogen, inorganic (PO_4) and total (tot-P) phosphorus and silicon dioxide (SiO_2) were determined, using a Lachat QuickChem 8000 autoanalyser (Lachat Instruments, Hach Co., Loveland, CO, USA) with the methods described in Hansen and Koroleff (1999). The concentrations of ammonium (NH_4) were determined manually, using a Genesys 10 spectrophotometer (Thermo Fisher Scientific Inc., Waltham, MA, USA). Since algae live in the concentrated brine and the concentrations of nutrients were measured from the melted bulk ice and slush, we normalized the concentrations of the nutrients to the under-ice water salinity, following Kaartokallio (2004), to reveal the salinity-independent changes.

Pigments

For pigment analyses, we filtered 100–206-ml subsamples on GF/F filters (Whatman, Sigma-Aldrich Co. LLC, St. Louis, MO, USA). We kept the filters at -80 °C until we sent them on dry ice to the Danish Hydraulic Institute (DHI; Hørsholm, Denmark) for analysis. At the DHI, the GF/F filters were transferred to vials with 3 ml 95% acetone with an internal standard (vitamin E). The samples were vortexed, sonicated on ice, extracted at +4 °C for 20 h and mixed again. The dissolved samples were then filtered through a 0.2 µm Teflon syringe filter into HPLC vials and placed in the cooling rack of the HPLC. Buffer (357 µl) and extract (143 µl) were injected into a Shimadzu LC-10 A HPLC system (DataApex Ltd., Prague, Czech Republic) with LC Solution software, using a pre-treatment program and mixing in the loop before injection. The HPLC method was that used byHooker et al. (2005) with the DHI internal method No.: SF No.: 30/852:01. In

addition to chl-*a*, other chlorophylls (chl-*b*, -c_1, -c_2, pheophytin *a*), PSCs (peridinin, fucoxanthin, neoxanthin, prasinoxanthin, alloxanthin) and PPCs (aphanizophyll, violaxanthin, myxoxanthophyll-like-1, diadinoxanthin, myxoxanthophyll-like-2, zeaxanthin, lutein, myxoxanthophyll-like-3, canthaxanthin, echinenone, β-carotene) were measured. Since our ice cores were melted overnight in darkness prior to extraction of the pigments, the pigments related to the xanthophyll cycle may have been enzymatically transformed into forms adapted to the dark conditions during the melting procedure (Claustre et al. 1994; Moline 1998). Our additional melting experiment verified that the PPCs disappeared from the samples more quickly than the PSCs and chlorophylls (Supplementary figure 2). Hence, we could not use the PPC:PSC ratios to consider the level of photoacclimation of the communities. The photosynthetic pigments, however, were not negatively affected by the melting time and were used here.

For comparison, we measured chl-*a* independently from each sample, using two 100-ml subsamples that we filtered onto GF/F filters, which we soaked in 96% v/v ethanol and kept in darkness overnight. We then filtered the ethanol through the GF/F filters to remove any particles and calculated the concentration of chl-*a* from the fluorescence that we measured with a Jasco FP-750 spectrofluorometer (Jasco Inc., Easton, MD, USA) calibrated with pure chl-*a* (HELCOM 1988). We presented the spectrofluorometer-measured chl-*a* results in association with primary production calculations for sea ice (Müller et al. 2016).

Light microscopy

For LM, we fixed 200-ml subsamples with glutaraldehyde (2% final concentration) and kept them in darkness at +6 °C until analysis. The organisms were enumerated with a Leica DMIL light microscope (Leica Microsystems GmbH, Wetzlar, Germany) in 50-ml subsamples settled according to Utermöhl (1958). Acid Lugol's solution (Willén 1962) was added to the glutaraldehyde-fixed samples just prior to the counting. The algal species with easily recognizable colony structure and

cell shape were identified at the species level, whereas the undetermined species were left at a general level, e.g. *Gymnodinium corollarium* A.M. Sundström, Kremp & Dauhbjerg, *Biecheleria baltica* Moestrup, Lindberg & Daugbjerg and *Scrippsiella hangoei* (J. Schiller) J. Larsen, with similar gross morphology, were identified as *Scrippsiella*-complex and the various euglenoid species as two size categories. Larger organisms were calculated with 10x/12.5 objectives from the entire cuvette bottom and smaller organisms with 40x/12.5 objectives from 120 grids distributed evenly over the cuvette bottom. The exception was the under-ice water sample at the drift-ice station, from which the smaller taxa were calculated from 60 grids distributed evenly over the cuvette bottom with 25x/12.5 and 40x/12.5 objectives. We converted the algal cell numbers into carbon biomasses (μg C l^{-1}), using species-specific biovolumes and carbon contents according to Olenina et al. (2006) and Menden-Deuer and Lessard (2000).

Molecular work

For the DNA extraction, we sequentially filtered 550–600-ml of water, melted sea ice and slush with 47-mm-diameter 180-μm pore-size nylon filters (Merck Millipore, Billerica, MA, USA), 20-μm polyvinylidene fluoride filters (Durapore©, Millipore), and 0.2-μm mixed-cellulose ester membrane filters (Schleicher and Schuell Bioscience GmbH, Dassel, Germany). We stored the 0.2-μm filters in liquid nitrogen while on board and transferred them to a -80 °C freezer ashore until further processing. We then soaked the 0.2-μm filters in DNA lysis buffer (100 mM Tris, 50 mM EDTA, 500 mM NaCl, 0.6% w/v SDS) and extracted the total DNA from each filter with the phenol-chloroform method (Maggs and Ward 1996).

Amplification and sequencing of the approximately 480-base pair (bp)-long 18S rRNA gene fragments (including the variable sites V7, V8 and V9) were carried out in two separate laboratories (the Research Center for Aquatic Genomics, Yokohama, Japan and the Institute of Biotechnology, Helsinki, Finland), using primers 18S-F1289 and 18S-R1772 (Nishitani et al. 2012) with attached

sample-specific 6-bp-long barcode tags, as described in Majaneva et al. (2015). The PCR products were mixed in equimolar ratios and a GS FLX Titanium Rapid Library Preparation Kit (Hoffmann-La Roche, Basel, Switzerland) was used to prepare a DNA library. These pooled libraries were then amplified with beads by emulsion PCR, and the amplified fragments in the DNA libraries were pyrosequenced on a picotitre plate with the 454 GS FLX Titanium system and reagents (Hoffmann-La Roche). We submitted the raw reads to the Sequence Read Archive of the European Nucleotide Archive (ENA) with accession number PRJEB7625.

We outlined the pyrosequencing results previously and used the total number of reads and operational taxonomic units (OTUs) for comparison of the various bioinformatic strategies (Majaneva et al. 2015). Here, we present the results in more detail. We processed the sequences in accordance with the QIIME Denoiser UCHIME pipeline (Majaneva et al. 2015), using QIIME 1.8.0 (Caporaso et al. 2010) and following the 454 Overview Tutorial and Analysis of the 18S data available in http://qiime.org/tutorials/index.html# (accessed January–March, 2014). To ensure favourable quality of the sequences, we eliminated those with more than six homopolymers, those with ambiguous bases, those with greater than zero mismatch in the barcode and primer sequence, and used the Denoiser (Reeder and Knight 2010) to further reduce the sequencing error rate. We identified chimeric reads, using UCHIME (Edgar et al. 2011). Our sample reads served as a reference. We removed reads occurring only once. We picked OTUs at the 97% similarity level, using the UCLUST method (Edgar 2010) in pick_otus.py. We generated taxonomic assignment of the 97% OTUs, using SILVA database release 111 (Quast et al. 2013) within the QIIME program package with UCLUST and the BLAST (Altschul et al. 1997). If UCLUST failed to assign the OTU, we used BLAST. In addition, we investigated common or ambiguously classified OTUs further, using BLASTn at the National Center for Biotechnology Information (NCBI). Once classified, we categorized the OTUs as phototrophs, heterotrophs or parasites, based on the

229 phylogenetic position of the specific taxa and available literature (see Supplementary file 1). For
230 downstream analyses, the number of reads per sample was normalized to 1354.

231 *Statistics*

232 To determine the general relationships, we used Spearman's ρ correlation to test the association
233 between two variables (pigment, LM and molecular results in different combinations). We
234 correlated the biomass and read abundance of some specific taxa, but not the total abundance of the
235 reads with chl-*a* or biomass, since research has shown that some taxa are overrepresented in
236 molecular studies, induced by different cell concentrations, biovolumes and co-occurring organisms
237 (e.g. Amacher et al. 2011). We chose Spearman's ρ, because it measures the extent to which the
238 other variable tends to increase or decrease as one variable increases, without requiring a linear
239 relationship. This is according to the philosophy that species may have non-linear relationships. We
240 used Dancey and Reidy's (2004) strength categorization: the correlation is strong when its value is
241 0.7–0.9 and moderate when 0.4–0.6. We also tested whether the number of OTUs and ratios of the
242 various accessory pigments to chl-*a* differed throughout the ice sections, using the one-way
243 ANOVA or non-parametric Kruskal-Wallis test (in the case when the variables were not normally
244 distributed, the Shapiro-Wilk test).

245 Furthermore, we investigated whether our samples were significantly grouped into two different *a*
246 *priori* groups: (1) *sample type*, including under-ice water, slush, drift ice, pack ice and fast ice and
247 (2) *vertical position*, including under-ice water, slush, surface ice, upper intermediate ice, middle
248 ice, lower intermediate ice and bottom ice. For these analyses, we used our LM, HPLC and
249 molecular taxonomic results individually and combined as variables in principal coordinate analysis
250 (PCoA) and following generalized discriminant analysis based on distances (CAP; Anderson and
251 Robinson 2003; Anderson and Willis 2003). We transformed the data to $y' = \ln(y + 1)$, and used
252 the Bray-Curtis dissimilarity (LM and HPLC, all data combined) or Jaccard dissimilarity (molecular

253 results) as a distance measure and let the CAP program determine the appropriate number of
254 dimensions (*m*) included in the discriminant analyses. OTUs that were observed more than once in a
255 minimum of two samples were included into the analysis to ensure sufficient data for ordination,
256 thus reducing the total number of OTUs from 221 to 118. For our molecular taxonomic results, we
257 chose a slightly modified approach for two reasons: (1) we used two different protocols to sequence
258 our samples, resulting in differing quality of these two data sets (see Majaneva et al. 2015) and (2)
259 the abundance of sequences was derived from the PCR amplification, which is not a real
260 abundance, but a compositional view. Only the molecular results showed significant grouping and
261 are presented here. In addition, we identified the OTUs that were responsible for the multivariate
262 patterns by considering the moderate and strong correlations of individual taxa with canonical axes
263 (86 OTUs).

264

265 **Results**

266 The mean (range) ice depth was 51 cm (43–66 cm), 82 cm (53–112 cm) and 55 cm (49.5–57.5 cm)
267 at the drift-ice, pack-ice and fast-ice stations, respectively. The mean snow depth was 7.5 cm, 5.5
268 cm and 5.5 cm at the respective stations. There was an additional, averaging 7.5-cm thick, layer of
269 slush between the snow and ice at the fast-ice station.

270 The surface and upper intermediate sections were mostly snow ice or transitional ice, while the
271 middle, lower intermediate and bottom sections were transitional or columnar ice at the fast-ice
272 station (Fig. 1a). The estimated brine volumes were 4.6–6.2 %, 4.0–8.0 % and 2.8–8.1 % at the
273 drift-ice, pack-ice and fast-ice stations, respectively (Fig. 1b).

274 The concentrations of NO_3+NO_2, NH_4 and tot-N were significantly higher in the fast ice than in the
275 drift and pack ice (repeated measures ANOVA, $p < 0.01$, followed by Tukey's pairwise

276 comparisons), while the concentrations of PO_4, tot-P and SiO_2 were similar among the stations
277 (Table 1). The nutrient concentrations in the ice were uniform vertically except for NH_4, which was
278 significantly higher in the surface ice than in the lower ice sections (mean in surface ice 15.77 µmol
279 l^{-1}, mean in lower ice sections 5.83 µmol l^{-1}, one-way ANOVA, $p < 0.01$, followed by Tukey's
280 pairwise comparisons). The molar ratios of NO_3+NO_2:SiO_2, NO_3+NO_2:PO_4 and SiO_2:PO_4 tended
281 towards phosphorus deficits in the slush, surface and upper intermediate ice sections
282 (NO_3:$Si(OH)_4$:PO_4 16:15:1; Brzezinski 1985; Redfield et al. 1963). The ratios were near optimal in
283 the lower intermediate and bottom sections of the pack-ice and fast-ice stations, but tended towards
284 nitrogen deficits in the lower ice sections of the drift ice. The PO_4 concentration was below the
285 detection limit only in the middle section of the pack ice and the upper intermediate section of the
286 fast ice, suggesting that algae had been actively consuming nutrients.

287 The concentration of chl-*a* was low in the under-ice water (0.5–1.0 µg l^{-1}; spectrofluorometer-
288 measured values; Müller et al. in press) and slush (0.5–1.6 µg l^{-1}). It was more variable within the
289 ice, ranging from 0.8 µg l^{-1} up to 13.8 µg l^{-1} (Fig. 2a–c). Fucoxanthin (0.021–6.438 µg l^{-1}, HPLC)
290 was the predominant accessory pigment, followed by pheophytin *a* (0–2.827 µg l^{-1}), chl-*b* (0.030–
291 0.574 µg l^{-1}), chl-c_1 (0–1.268 µg l^{-1}), chl-c_2 (0–0.754 µg l^{-1}), peridinin (0.023–1.278 µg l^{-1}),
292 diadinoxanthin (0.014–1.673 µg l^{-1}) and β-carotene (0.001–0.404 µg l^{-1}) (Fig. 2a–c; Supplementary
293 table 1).

294 The concentrations of the accessory pigments combined in our samples correlated strongly with the
295 concentrations of chl-*a* (Spearman's $\rho = 0.917$, $p < 0.001$), and the accessory pigments to chl-*a*
296 ratios were constant throughout the sea ice (median 0.79; Kruskal-Wallis test, $p > 0.05$; Fig. 2d–f).
297 An exception was the bottom-ice section of the pack ice, where the concentration of pheophytin *a*
298 (2.827 µg l^{-1}) was higher than that of chl-*a* (2.425 µg l^{-1}; discussed below in association with
299 potential herbivory). The chl-*b*+*c*:chl-*a*, carotenoids:chl-*a*, PSC:chl-*a* and fucoxanthin:chl-*a* ratios

were also constant throughout the sea ice (Kruskal-Wallis test, $p > 0.05$), showing no vertical adjustment of the photosynthetic pigment pool.

The biomass of the algae correlated strongly with the concentration of chl-*a* (Spearman's $\rho = 0.829$, $p < 0.001$). The biomass was higher in the slush (12–44 µg C l^{-1}) than in the under-ice water (2–8 µg C l^{-1}; Fig. 2a,c). In the sea ice, the biomass was highly variable (13–110 µg C l^{-1}), and the highest biomasses were in the bottom (60 µg C l^{-1}; Fig. 2a), middle (46 µg C l^{-1}; Fig. 2b) and upper intermediate (110 µg C l^{-1}; Fig. 2c) sections of the drift ice, pack ice and fast ice, respectively.

The number of OTUs (Table 1) did not correlate ($p > 0.05$) with either the concentration of chl-*a* or the LM-enumerated biomass of algae, suggesting that the OTU richness was not related to algal biomass in the sea ice. The number of OTUs was higher in the under-ice water than in the sea ice and slush (mean 107, 70 and 53, respectively; one-way ANOVA, $p < 0.01$, followed by Tukey's pairwise comparisons). PCoA of the molecular community composition separated the under-ice water and slush samples from the ice samples. The following discriminant analysis revealed that there were also significant differences in the drift-ice, pack-ice and fast-ice communities ($\delta^2_1 = 0.978$, $\delta^2_2 = 0.944$, $t_2 = 3.55$, $p < 0.001$, 9999 permutations, mis-classification error 5%, Fig. 3). The differences among the communities arose mainly from the various phagotrophic protistan taxa inhabiting the communities, as observed in older sea ice in the Antarctic (Stoecker et al. 1993). Slush especially was characterized by the presence of phagotrophic protists; only 18 % of the OTUs correlating with slush were phototrophic while 37 % of those correlating with the under-ice water and 49 % of those correlating with ice were phototrophs (Fig. 3). Overall, 36 % of the OTUs were phototrophs in our data set (Supplementary file 1).

The centric diatom *Melosira arctica* Dickie bloomed in the upper intermediate section (11–22 cm) at the fast-ice station, with a particularly high biomass of over 76 µg C l^{-1} (Fig. 4c; Supplementary table 2). At the pack-ice station, *Melosira arctica* also showed the highest biomass in the upper

intermediate section (Fig. 4b; 11.6 µg C l^{-1}; 16–32 cm) together with small, 6–10-µm, unidentified centric diatoms (10.2 µg C l^{-1}, probably *Thalassiosira* Cleve species, OTU 252; Fig. 5b). Overall, centric diatoms were more abundant than pennate diatoms in our sea-ice samples, except in the bottom section (ice depth 44–55 cm) at the fast-ice station, where the pennate *Pauliella taeniata* (Grunow) F.E. Round & Basson had the highest biomass (4.5 µg C l^{-1}).

In terms of biomass, unidentified dinoflagellates smaller than 20 µm were the most abundant dinoflagellates (Fig. 4a–c; Supplementary table 2). The biomass of these dinoflagellates correlated moderately with the read abundance of *Heterocapsa arctica* Horiguchi subsp. *frigida* Rintala & G. Hällfors (OTU 64; Spearman's $\rho = 0.59$, $p < 0.01$; Fig. 5), a species that was not recognized in microscopic counts, but that was one of the four most abundant dinoflagellate OTUs present in all samples. The other three dinoflagellate OTUs present in all of our samples were affiliated with *Scrippsiella hangoei* (OTU 112; Supplementary file 1), *Biecheleria baltica* (OTU 268) and *Gymnodinium corollarium* (OTU 184), which are difficult to separate under LM. These three species are commonly found in ice and begin their spring bloom in the under-ice water (Spilling 2007; Sundström et al. 2009). Here, *Biecheleria baltica* correlated strongly with sea ice (Fig. 3), but when we used the abundance of the reads indicatively, *Scrippsiella hangoei* was the most abundant species in our samples. Exceptions occurred in the middle and lower intermediate sections of the pack ice, where *Biecheleria baltica* was the most abundant species (Fig. 5b), and the three species showed the highest biomass (middle section of the pack ice 2.7 µg C l^{-1}; Fig. 4b).

Cercozoans constituted 20% of the OTU richness, and their read abundance was highest in the surface-ice sections, drift-ice bottom section and slush (Fig. 5a-c; Supplementary file 1), but their reads may have been overrepresented, due to high pyrosequencing error rates in Cercozoa (Behnke et al. 2011). However, *Cryothecomonas* Thomsen Buck, Bolt & Garrison and *Protaspis* Skuja species have shown clear preference for the ice habitat (Ikävalko and Thomsen 1997; Thaler and

348 Lovejoy 2012; Vørs 1992). Here, the various *Cryothecomonas*, *Protaspis* and *Protaspa* Cavalier-
349 Smith OTUs were characteristic of slush and ice, while being rare in the under-ice water (Fig. 3;
350 Supplementary file 1). Most of the cercozoan OTUs were classified only to a higher taxonomic
351 level, and their identity and potential role remain obscure (Supplementary file 1).

352 The unidentified flagellates had the highest biomass in slush (Fig. 4c; 65 % of algal biomass).
353 Based on our molecular results, these algae were affiliated with two *Ochromonas* Vysotskii species
354 (OTUs 287 and 92; Supplementary file 1), *Pyramimonas gelidicola* McFadden, Moestrup &
355 Wetherbee (OTU 171), *Aureococcus* P.E. Hargraves & P.W.Sieburth species (OTU 108) and
356 *Chlamydomonas pulsatilla* H.W. Wollenweber (OTU 288). However, these OTUs were also present
357 in sea ice and did not correlate with the slush (Fig. 3). The green algae *Mantoniella squamata*
358 (Manton & Parke) Desikachary (OTU 15), *Chlamydomonas* Ehrenberg (OTU 109) and
359 *Chlamydomonas pulsatilla* (OTU 288), on the other hand, correlated moderately with the sea ice
360 (Fig. 3). The under-ice water and sea ice harboured different cryptomonad species, based on our
361 molecular results. *Teleaulax amphioxeia* (W. Conrad) D.R.A. Hill (OTU 44) was characteristic of
362 the under-ice water, while *Hemiselmis* M.W. Parke (OTU 194), *Chroomonas* Hansgirg (OTU 125)
363 and *Falcomonas* D.R.A. Hill (OTU 167) were characteristic of the sea-ice. Other characteristic sea-
364 ice flagellates included the haptophyte *Isochrysis* M. Parke species (OTU 85), *Goniomonas* Stein
365 species (OTU 253), *Nannochloropsis limnetica* L. Krienitz, D. Hepperle, H.-B. Stich & W. Weiler
366 (OTU 259), two *Paraphysomonas* De Saedeleer species (OTUs 32 and 133) and two unaffiliated
367 chrysophytes (OTUs 30 and 134).

368 The high biomass of the cyanobacterium *Aphanizomenon* A. Morren ex É. Bornet & C. Flahault sp.
369 (e.g. 22.1 µg C l^{-1} in the bottom section of the drift ice; Fig. 4a) is a genuine peculiarity of Baltic
370 Sea ice. Niemi (1973) already reported that *Aphanizomenon* sp. is abundant in the Baltic Sea during
371 winter. It tolerates salinities of only up to 10 (Lehtimäki et al. 1997), and therefore the high biomass

372 of *Aphanizomenon* sp. in sea ice indicates the presence of low-salinity brine during the time of
373 biomass accumulation.

374 Ciliates were rarely observed in LM, but *Strombidium* Claparède & Lachmann species showed
375 measurable biomass (2.3–5.3 µg C l^{-1}; Fig. 6c, Supplementary table 2) in slush. Based on our
376 molecular results, these were cells of mixotrophic *Strombidium biarmatum* Agatha, Strüder-Kypke,
377 Beran & Lynn (Spearman's $\rho = 0.640$, $p < 0.01$, OTU 241; Fig. 6d, Supplementary file 1; Agatha et
378 al. 2005). The presence of pheophytin *a* and higher biomass of ciliates coincided in the lower
379 intermediate and bottom sections of the drift ice (pheophytin *a*: 0.4–0.5 µg l^{-1}, biomass: 3.1 µg C l^{-1};
380 Fig. 6a), suggesting ciliate herbivory. The most abundant OTUs in these samples were affiliated
381 with *Phialina* Bory de Saint Vincent (OTU 12; Fig. 6d, Supplementary file 1), *Homalogastra setosa*
382 Kahl (OTU 116), *Balanion* Wulff (OTU 31) and *Rimostrombidium veniliae* (Montagnes & Taylor)
383 Petz, Song & Wilbert (OTU 62). *Lacrymaria rostrata* Kahl or *Lacrymaria* Ehrenberg sp. have been
384 commonly reported in Baltic Sea ice (e.g. Kaartokallio et al. 2007; Rintala et al. 2010, our LM), but
385 these ciliates belong to the genus *Phialina* rather than to the genus *Lacrymaria*, based on our
386 molecular results (OTUs 65 and 12 in Supplementary file 1, Spearman's $\rho = 0.476$, $p < 0.05$).

387

388 **Discussion**

389 The ice-algal communities studied were in the early-blooming stage, considering the sampling
390 season, brine volumes, nutrient concentrations and biomass of organisms (Kuosa and Kaartokallio
391 2006; Piiparinen et al. 2010). The algae were not limited by space, since most of our ice sections
392 had brine volumes over 5 %, which is the threshold at which brine channels become interconnected
393 (Golden et al. 1998). On average, the brine volume of Baltic Sea ice is lower, 1.5–3.5 % (Granskog
394 et al. 2006), and such low brine volumes restrict to some degree the biomass in sea ice (Piiparinen

et al. 2010). Similarly, the ice algae were hardly nutrient limited, since the relatively high concentrations of salinity-normalized nutrients were measured from bulk ice and algae live in the concentrated brine. The uniform accessory pigments to chl-*a* ratios vertically indicated that the algae, as a community, did not adjust the photosynthetic pigment pool vertically or contain more accessory photosynthetic pigments deeper in the ice and were not shade adapted. The weak shade adaptation and the time of sampling also suggest that the ice algae were likewise not limited by light (Kuosa and Kaartokallio 2006).

The weak shade adaptation is in contrast to the results from polar regions (Alou-Font et al. 2013; Arrigo et al. 2014), where the accessory pigment composition and accessory pigments to chl-*a* ratios reflected acclimation to available light. In comparison to arctic and antarctic sea ice (Alou-Font et al. 2013; Arrigo et al. 2014), the relatively thin ice and snow cover of the Baltic Sea, as well as our time of sampling, may explain why there was no vertical change in the photosynthetic accessory pigments. This is supported by the light saturation index (E_k), which did not tend to decrease downwards (Müller et al. in press), albeit the 5.3–7.5-cm snow cover at our collecting sites was sufficient to attenuate 80% of the incident radiation (Müller et al. in press). The E_k values in our samples were also higher than those in previous Baltic Sea measurements (Enberg et al. 2015; Piiparinen and Kuosa 2011; Piiparinen et al. 2010; Rintala et al. 2010). Nevertheless, all the Baltic E_k values measured are more comparable to values under thin-ice conditions than to values under low-light conditions (Ban et al. 2006; Obata and Taguchi 2009; Robinson et al. 1998), and Baltic Sea bottom-ice algae are not as shade-adapted as the bottom-ice algae in polar regions (Alou-Font et al. 2013; Arrigo et al. 2014). Within the thinner Baltic Sea ice, there is simply more light available for the bottom-ice algae than within the thicker polar sea ice.

Presumably, the light conditions were also more favourable for centric than pennate diatoms, considering P-E curves (Müller et al. 2016) and the fact that centric diatoms are not as shade

419 adapted as pennate diatoms (Piiparinen et al. 2010). The centric *Melosira arctica* exploits the light
420 available in the Baltic surface ice and forms dense blooms, especially if there is space and nutrients
421 (Kuosa and Kaartokallio 2006; Piiparinen et al. 2010; Rintala et al. 2010). Thus, the dominance of
422 pennate diatoms in the Baltic Sea ice (Haecky and Andersson 1999; Haecky et al. 1998; Huttunen
423 and Niemi 1986; Ikävalko and Thomsen 1997) is not predetermined, and diatom blooms are not
424 restricted to the bottom ice.

425 Ciliates have been identified as key herbivores in Baltic Sea ice (Kaartokallio 2004; Kaartokallio et
426 al. 2007; Rintala et al. 2006, 2010). Here, the ciliate biomass was low and ciliate reads were
427 probably overrepresented, due to high gene copy numbers, large biovolumes and preferential primer
428 binding of alveolates (Amacher et al. 2011; Zhu et al. 2005), as well as possible amplification of
429 dormant cysts. The absence of pheophytin *a* (Fig. 6c, Supplementary table 1), an indicator for
430 herbivory (Prins et al. 1991; Strom 1993; Szymczak-Zyła et al. 2008), from most of the samples
431 supports the view that ciliates were rare in our samples. The most abundant ciliates encountered
432 here – *Strombidium* species – are also known for their capability for sequestering viable
433 chloroplasts from their algal prey and using them to acquire phototrophy (Stoecker et al. 2009).
434 Thus, the slush samples were not experiencing high rates of herbivory, even though the
435 *Strombidium* biomass and read abundance were high.

436 In contrast, we found evidence for ciliate herbivory in drift ice, where the presence of pheophytin *a*,
437 higher ciliate biomass and herbivorous *Homalogastra* Kahl, *Balanion* and *Rimostrombidium*
438 (Fauré-Fremiet) Jankowski (Kahl 1926; Kim et al. 2007; Liu et al. 2012) OTUs coincided.
439 Glutaraldehyde and Lugol's solution are known to cause up to 70% shrinkage of ciliates (Choi and
440 Stoecker 1989; Jerome et al. 1993). Consequently, *Homalogastra*, *Balanion* and *Rimostrombidium*
441 species were the clearest candidates for ice algal grazers in the drift ice, although they are > 25 µm
442 in size (Kahl 1926; Kim et al. 2007; Liu et al. 2012), while the most abundant ciliates in the drift-ice

443 samples were < 10 µm (Fig. 6a, Supplementary table 2). In the upper intermediate section of the
444 fast ice, pheophytin *a* originated more probably from senescent blooming *Melosira arctica* cells
445 than from herbivory (Louda et al. 1998). Likewise, the high concentration of pheophytin *a* at the
446 bottom of the pack ice (2.8 µg l^{-1}; Fig. 6b, Supplementary table 1), with no metazoans or ciliates
447 encountered in LM and low ciliate read abundance (Fig. 6e; Supplementary tables 2 and 3), could
448 have indicated the presence of senescent cells. However, the copepod *Eurytemora affinis* Poppe
449 reads were abundant in pack ice (Fig. 5b, Supplementary file 1), and a single copepodid stage IV
450 *Eurytemora affinis* was found in the surface section of the pack ice, implying that this common
451 Baltic Sea copepod was present as living individuals in the pack ice and perhaps responsible for the
452 herbivory in the bottom-ice section of the pack ice.

453 In conclusion, we showed that Baltic Sea ice algae do not adjust the photosynthetic pigment pool
454 vertically and thus are not shade-adapted in the early-blooming stage in March, and we lent support
455 to the view that centric diatoms are equally as important in Baltic Sea ice as are pennate diatoms
456 and may bloom in any section of the ice. Based on our results, phototrophs preferred sea ice and
457 were present in various types of ice, while various phagotrophic taxa were characteristic of the sea-
458 ice, slush and under-ice water communities. Lastly, the presence of pheophytin *a* coincided with
459 elevated ciliate biomass and high read abundance of three herbivorous ciliate OTUs in the drift ice
460 and high read abundance of *Eurytemora affinis* in the pack ice, indicating that the ciliates and
461 *Eurytemora affinis* were grazing on the ice algae.

462

463 **Acknowledgements**

464 The Walter and Andrée de Nottbeck Foundation funded the materials and logistics, as well as the
465 work, of Markus Majaneva, Janne-Markus Rintala and Susann Müller. The Onni Talas Foundation

466 funded the work of Sanna Majaneva and Kirsi Hyytiäinen. The work by Markus Majaneva and
467 Kirsi Hyytiäinen was funded by Helsinki University Three-Year Research Grants (Blomster). We
468 are grateful to Jari Haapala, the cruise leader of the R/V Aranda sea-ice cruise 2010. We would also
469 like to thank Atushi Fujiwara and Yasuike Motoshige for their molecular laboratory work, Ilkka
470 Lastumäki for the nutrient analyses, Ilkka Matero for the ice-structure analyses, Johanna Oja for
471 LM and James Thompson for the language check. Finally, we would like to thank Jacob Larsen for
472 the original idea of measuring the accessory pigments in sea ice.

473

474 **Appendix A. Supplementary data**

475 The supplementary data associated with this article can be found, in the online version, at http://...

476

477 **References**

478 Agatha, S., Strüder-Kypke, M.C., Beran, A., Lynn, D.H., 2005. *Pelagostrobilidium neptuni*
479 (Montagnes and Taylor, 1994) and *Strombidium biarmatum* nov. spec. (Ciliophora,
480 Oligotrichea): phylogenetic position inferred from morphology, ontogenesis, and gene
481 sequence data. Eur. J. Protistol. 41, 65–83.

482 Alou-Font, E., Mundy, C-J., Roy, S., Gosselin, M., Agustí, S., 2013. Snow cover affects ice algal
483 pigment composition in the coastal Arctic Ocean during spring. Mar. Ecol. Prog. Ser. 474,
484 89–104.

485 Altschul, S.F., Madden, T.L., Schäffer, A.A., Zhang, J., Zhang, Z., Miller, W., Lipman, D.J., 1997.
486 Gapped BLAST and PSI-BLAST: a new generation of protein database search programs.
487 Nucleic Acids Res. 25, 3389–3402.

488 Amacher, J.A., Baysinger, C.W., Neuer, S., 2011. The importance of organism density and co-
489 occurring organisms in biases associated with molecular studies of marine protist diversity. J.
490 Plankton Res. 33, 1762–1766.

491 Anderson, M.J., Robinson, J., 2003. Generalized discriminant analysis based on distances. Aust. N.
492 Z. J. Stat. 45, 301–318.

493 Anderson, M.J., Willis, T.J., 2003. Canonical analysis of principal coordinates: a useful method of
494 constrained ordination for ecology. Ecology 84, 511–525.

495 Arrigo, K.R., Brown, Z.W., Mills, M.M., 2014. Sea ice algal biomass and physiology in the
496 Amundsen Sea, Antarctica. Elem. Sci. Anth. 2, 000028.

497 Ban, A., Aikawa, S., Hattori, H., Sasaki, H., Sampei, M., Kudoh, S., Fukuchi, M., Satoh, K.,
498 Kashino, Y., 2006. Comparative analysis of photosynthetic properties in ice algae and
499 phytoplankton inhabiting Franklin Bay, the Canadian Arctic, with those in mesophilic
500 diatoms during CASES 03–04. Polar Biosci. 19, 11–28.

501 Behnke, A., Engel, M., Christen, R., Nebel, M., Klein, R.R., Stoeck, T., 2011. Depicting more
502 accurate pictures of protistan community complexity using pyrosequencing of hypervariable
503 SSU rRNA gene regions. Environ. Microbiol. 13, 340–349.

504 Bidigare, R.R., Van Heukelem, L., Trees, C.C., 2005. Analysis of algal pigments by high-
505 performance liquid chromatography. In: Andersen, R.A., (Ed.), Algal culturing techniques.
506 Elsevier Academic Press, Amsterdam, pp. 327−345.

507 Brzezinski, M.A., 1985. The Si: C: N ratio of marine diatoms: interspecific variability and the effect
508 of some environmental variables. J. Phycol. 21, 347−357.

509 Caporaso, J.G., Kuczynski, J., Stombaugh, J., Bittinger, K., Bushman, F.D., Costello, E.K., Fierer,
510 N., Peña, A.G., Goodrich, J.K., Gordon, J.I., Huttley, G.A., Kelley, S.T., Knights, D., Koenig,
511 J.E., Ley, R.E., Lozupone, C.A., McDonald, D., Muegge, B.D., Pirrung, M., Reeder, J.,
512 Sevinsky, J.R., Turnbaugh, P.J., Walters, W.A., Widmann, J., Yatsunenko, T., Zaneveld, J.,
513 Knight, R., 2010. QIIME allows analysis of high-throughput community sequencing data.
514 Nat. Methods 7, 335–336.

515 Caron, D.A., Countway, P.D., Savai, P., Gast, R.J., Schnetzer, A., Moorthi, S.D., Dennett, M.R.,
516 Moran, D.M., Jones, A.C., 2009. Defining DNA-based operational taxonomic units for
517 microbial-eukaryote ecology. Appl. Environ. Microbiol. 75, 5797–5808.

518 Choi, J.W., Stoecker, D.K., 1989. Effects of Fixation on Cell Volume of Marine Planktonic
519 Protozoa. Appl. Environ. Microbiol. 55, 1761–1765.

520 Claustre, H., Kerherve, P., Marty, J.C., Prieur, L., 1994. Phytoplankton photoadaptation related to
521 some frontal physical processes. J. Mar. Sci. 5, 251–265.

522 Comeau, A.M., Philippe, B., Thaler, M., Gosselin, M., Poulin, M., Lovejoy, C., 2013. Protists in
523 Arctic drift and land-fast sea ice. J. Phycol. 49, 229–240.

524 Cox, G.F.N., Weeks, W.F., 1983. Equations for determining the gas and brine volumes in sea-ice
525 samples. J. Glaciol. 29, 306–316.

526 Dancey, C., Reidy, J., 2004. Statistics Without Maths for Psychology: Using SPSS for Windows.
527 Prentice Hall, London.

528 Edgar, R.C., 2010. Search and clustering orders of magnitude faster than BLAST. Bioinformatics
529 26, 2460–2461.

530 Edgar, R.C., Haas, B.J., Clemente, J.C., Quince, C., Knight, R., 2011. UCHIME improves
531 sensitivity and speed of chimera detection. Bioinformatics 27, 2194–2200.

532 Eicken, H., Lensu, M., Leppäranta, M., Tucker III, W.B., Gow, A.J., Salmela, O., 1995. Thickness,
533 structure, and properties of level summer multi-year ice in the Eurasian sector of the Arctic
534 Ocean. J. Geophys. Res. 100, 22697–22710.

535 Enberg, S., Piiparinen, J., Majaneva, M., Vähätalo, A.V., Autio, R., Rintala, J-M., 2015. Solar PAR
536 and UVR modify the community composition and the photosynthetic activity of sea ice algae.
537 FEMS Microbiol. Ecol. 91, fiv102.

538 Golden, K.M., Ackley, S.F., Lytle, V.I., 1998. The percolation phase transition in sea ice. Science
539 282, 2238–2241.

540 Granskog, M., Kaartokallio, H., Kuosa, H., Thomas, D.N., Vainio, J., 2006. Sea ice in the Baltic
541 Sea – A review. Estuar. Coast. Shelf Sci. 70, 145–160.

542 Haecky, P., Andersson, A., 1999. Primary and bacterial production in sea ice in the northern Baltic
543 Sea. Aquat. Microb. Ecol. 20, 107–118.

544 Haecky, P., Jonsson, S., Andersson, A., 1998. Influence of sea ice on the composition of the spring
545 phytoplankton bloom in the northern Baltic Sea. Polar Biol. 20, 1–8.

546 Hällfors, G., Niemi, Å., 1974. A *Chrysochromulina* (Haptophyceae) bloom under the ice in the
547 Tvärminne archipelago, southern coast of Finland. Mem. Soc. Fauna Flora Fenn. 50, 89–104.

548 Hansen, H.P., Koroleff, F., 1999. Determination of nutrients. In: Grasshoff, K., Kremling, K.,
549 Ehrhardt, M., (Eds.), Methods of Seawater Analysis, 3rd edn. Verlag Chemie Gmbh,
550 Weinhheim, pp. 159–228.

551 Häyren, E., 1929. Zwei notizen über das Meereseis und die Algen. Mem. Soc. Fauna Flora Fenn. 5,
552 134–140.

553 HELCOM, 1988. Guidelines for the Baltic monitoring programme for the third stage; Part D.
554 Biological determinants. Balt. Sea Environ. Proc. 27D, 16–23.

555 Hickel, W., 1969. Planktologische und hydrographisch-chemische Untersuchungen in der
556 Eckernfördern Bucht (Wesliche Ostsee) 1962/1963 Helgoland. Wiss. Meer. 19, 318–331.

557 Hooker, S.B., Van Heukelem, L., Thomas, C.S., Claustre, H., Ras, J., Barlow, R., Sessions, H.,
558 Schlüter, L., Perl, J., Trees, C., Stuart, V., Head, E., Clementson, L., Fishwick, J., Llewellyn,
559 C., Aiken, J., 2005. The second SeaWiFS HPLC Analysis Round-Robin Experiment
560 (SeaHARRE-2), NASA, Goddard Space Flight Center, Maryland, Technical Memorandum
561 NASA/TM-2005-212787.

562 Huttunen, M., Niemi, Å., 1986. Sea-ice algae in the Northern Baltic Sea. Mem. Soc. Fauna Flora
563 Fenn. 62, 58–62.

564 Ikävalko, J., 1998. Further observations on flagellates within sea ice in northern Bothnian Bay, the
565 Baltic Sea. Polar Biol. 19, 323–329.

566 Ikävalko, J., Thomsen, H.A., 1996. Scale-covered and loricate flagellates (Chrysophyceae and
567 Synurophyceae) from the Baltic Sea ice. Nova Hedwigia Beih. 114, 147–160.

568 Ikävalko, J., Thomsen, H.A., 1997. The Baltic Sea ice biota (March 1994): a study of the protistan
569 community. Eur. J. Protistol. 33, 229–243.

570 Jeffrey, S.W., Wright, S.W., Zapata, M., 2011. Microalgal classes and their signature pigments. In:
571 Roy, S., Llewellyn, C.A., Egeland, E.S., Johnsen, G., (Eds.), Phytoplankton Pigments:
572 Characterization, Chemotaxonomy and Applications in Oceanography, Cambridge University
573 Press, Cambridge, pp. 3–77.

574 Jerome, C.A., Montagnes, D.J.S., Taylor, F.J.R., 1993. The effect of the quantitative protargol stain
575 and Lugol's and Bouin's fixatives on cell size: a more accurate estimate of ciliate species
576 biomass. J. Euk. Microbiol. 40, 253–259.

577 Kaartokallio, H., 2004. Food web components, and physical and chemical properties of Baltic Sea
578 ice. Mar. Ecol. Prog. Ser. 273, 49–83.

579 Kaartokallio, H., Kuosa, H., Thomas, D.N., Granskog, M.A., Kivi, K., 2007. Biomass, composition
580 and activity of organism assemblages along a salinity gradient in sea ice subjected to river
581 discharge in the Baltic Sea. Polar Biol. 30, 183–197.

582 Kahl, A., 1926. Neue und wenig bekannte Formen der holotrichenund heterotrichen Ciliaten. Arch.
583 Protistenkd. 55, 198–438.

584 Kim, J.S., Jeong, H.J., Lynn, D.H., Park, J.Y., Lim, Y.W., Shim, W., 2007. *Balanion masanensis* n.
585 sp. (Ciliophora: Prostomatea) from the coastal waters of Korea: morphology and small
586 subunit ribosomal RNA gene sequence. J. Euk. Microbiol. 54, 482–494.

587 Kudoh, S., Imura, S., Kashino, Y., 2003. Xanthophyll-cycle of ice algae on the sea ice bottom in
588 Saroma Ko lagoon, Hokkaido, Japan. Polar Biosci. 16, 86–97.

589 Kuosa, H., Kaartokallio, H., 2006. Experimental evidence on nutrient and substrate limitation of
590 Baltic Sea sea-ice algae and bacteria. Hydrobiologia 554, 1–10.

591 Lehtimäki, J., Moisander, P., Sivonen, K., Kononen, K., 1997. Growth, nitrogen fixation, and
592 nodularin production by two Baltic Sea cyanobacteria. Appl. Environ. Microbiol. 63, 1647–
593 1656.

594 Leppäranta, M., Manninen, T., 1988. The brine and gas content of sea ice with attention to low
595 salinities and high temperatures. Internal Rep 88-2, Finnish Institute of Marine Research,
596 Helsinki.

597 Liu, W., Yi, Z., Lin, X., Warren, A., Song, W., 2012. Phylogeny of three choreotrich genera
598 (Protozoa, Ciliophora, Spirotrichea), with morphological, morphogenetic and molecular
599 investigations on three strobilidiid species. Zool. Scr. 41, 417–434.

600 Logares, R., Audic, S., Santini, S., Pernice, M.C., de Vargas, C., Massana, R., 2012. Diversity
601 patterns and activity of uncultured marine heterotrophic flagellates unveiled with
602 pyrosequencing. ISME J. 6, 1823–1833.

603 Louda, J.W., Li, J., Liu, L., Winfree, N., Baker, E.W., 1998. Chlorophyll-a degradation during
604 cellular senescence and death. Org. Geochem. 29, 1233–1251.

605 Lowe, C.D., Keeling, P.J., Martin, L.E., Slamovits, C.H., Watts, P.C., Montagnes, D.J.S., 2011.
606 Who is *Oxyrrhis marina*? Morphological and phylogenetic studies on an unusual
607 dinoflagellate. J. Plankton Res. 33, 555–567.

608 Maggs, C.A., Ward, B.A., 1996. The genus *Pikea* (Dumontiaceae, Rhodophyta) in England and the
609 North Pacific: comparative morphological, life history, and molecular studies. J. Phycol. 32,
610 176–193.

611 Majaneva, M., Rintala, J-M., Piisilä, M., Fewer, P.D., Blomster, J., 2012. Comparison of wintertime
612 nano-sized eukaryotic communities in the Baltic Sea ice and water, based on sequencing of
613 the 18S rRNA gene. Polar Biol. 35, 875–889.

614 Majaneva, M., Hyytiäinen, K., Varvio, S.L., Nagai, S., Blomster, J., 2015. Bioinformatic amplicon
615 read processing strategies strongly affect eukaryotic diversity and the taxonomic composition
616 of communities. PLoS ONE 10, e0130035.

617 Meiners, K., Fehling, J., Granskog, M.A., Spindler, M., 2002: Abundance, biomass and
618 composition of biota in Baltic Sea ice and underlying water (March 2000). Polar Biol. 25,
619 761–770.

620 Menden-Deuer, S., Lessard, E.J., 2000. Carbon to volume relationships for dinoflagellates, diatoms,
621 and other protist plankton. Limnol. Oceanogr. 45, 569–79.

622 Moline, M.A., 1998. Photoadaptive response during the development of a coastal Antarctic diatom
623 bloom and relationship to water column stability. Limnol. Oceanogr. 43, 146–153.

624 Müller, S., Uusikivi, J., Vähätalo, A.V., Majaneva, M., Majaneva, S., Autio, R., Rintala, J-M.,
625 2016. Primary production calculations for sea ice from bio-optical observations in the Baltic
626 Sea. Elem. Sci. Anth. 4, 000121.

627 Niemi, Å., 1973. Ecology of phytoplankton in the Tvärminne area, SW coast of Finland. I
628 Dynamics of hydrography, nutrients, chlorophyll a and phytoplankton. Acta Bot. Fenn. 100,
629 1–68.

630 Nishitani, G., Nagai, S., Hayakawa, S., Kosaka, Y., Sakurada, K., Kamiyama, T., Gojobori, T.,
631 2012. Multiple plastids collected by the dinoflagellate *Dinophysis mitra* through
632 kleptoplastidy. Appl. Environ. Microbiol. 78, 813–821.

633 Norrman, B., Andersson, A., 1994. Development of ice biota in a temperate sea area (Gulf of
634 Bothnia). Polar Biol. 14, 531–537.

635 Obata, M., Taguchi, S., 2009. Photoadaptation of an ice algal community in thin sea ice, Saroma-ko
636 Lagoon, Hokkaido, Japan. Polar Biol. 32, 1127–1135.

637 Olenina, I., Hajdu, S., Edler, L., Andersson, A., Wasmund, N., Busch, S., Göbel, J., Gromisz, S.,
638 Huseby, S., Huttunen, M., Jaanus, A., Kokkonen, P., Ledaine, I., Niemkiewicz, E., 2006.
639 Biovolumes and size-classes of phytoplankton in the Baltic Sea. Balt. Sea Environ. Proc. 106,
640 1–144.

641 Palosuo, E., 1961. Crystal structure of brackish and freshwater ice. IASH 54, 9–14.

642 Petrich, C., Eicken, H., 2010. Growth, structure and properties of sea ice. In: Thomas, D.N.,
643 Dieckmann, G.S., (Eds.), Sea ice – second edition, Blackwell Publishing Ltd, Oxford, pp. 23–
644 77.

645 Piiparinen. J., Kuosa, H., 2011. Impact of UVA radiation on algae and bacteria in Baltic Sea ice.
646 Aquat. Microb. Ecol. 63, 75−87.

647 Piiparinen, J., Kuosa, H., Rintala, J-M., 2010. Winter-time ecology in the Bothnian Bay, Baltic Sea:
648 nutrients and algae in fast ice. Polar Biol. 33, 1445−1461.

649 Prins, T.C., Smaal, A.C., Pouwer, A.J., 1991. Selective ingestion of phytoplankton by the bivalves
650 *Mytilus edulis* L. and *Cerastoderma edule* (L.). Hydrobiol. Bull. 25, 93–100.

651 Quast, C., Pruesse, E., Yilmaz, P., Gerken, J., Schweer, T., Yarza, P., Peplies, J., Glöckner, F.O.,
652 2013. The SILVA ribosomal RNA gene database project: improved data processing and web-
653 based tools. Nucleic Acids Res. 41, D590–D596.

654 Redfield, A.C., Ketchum, B.H., Richards, F.A., 1963. The influence of organisms on the
655 composition of sea-water. In: Hill, M.N., (Ed.), The sea, Vol 2. Interscience, New York, pp.
656 26−77.

657 Reeder, J., Knight, R., 2010. Rapidly denoising pyrosequencing amplicon reads by exploiting rank-
658 abundance distributions. Nat. Methods 7, 668–669.

659 Rintala, J-M., Piiparinen, J., Ehn, J., Autio, R., Kuosa, H., 2006. Changes in phytoplankton biomass
660 and nutrient quantities in sea ice as responses to light/dark manipulations during different
661 phases of the Baltic winter 2003. Hydrobiologia 554, 11–24.

662 Rintala, J-M., Piiparinen, J., Uusikivi, J., 2010. Drift-ice and under-ice water communities in the
663 Gulf of Bothnia (Baltic Sea). Polar Biol. 33, 179–191.

664 Rintala, J-M., Piiparinen, J., Blomster, J., Majaneva, M., Müller, S., Uusikivi, J., Autio, R., 2014.
665 Fast direct melting of brackish sea-ice samples results in biologically more accurate results
666 than slow buffered melting. Polar Biol. 37, 1811–1822.

667 Robinson, D.H., Arrigo, K.R., Kolber, Z., Gosselin, M., Sullivan, C.W., 1998. Photophysiological
668 evidence of nutrient limitation of platelet ice algae in McMurdo Sound, Antarctica. J. Phycol.
669 34, 788–797.

670 Sinha, N.K., 1977. Technique for studying structure of sea ice. J. Glaciol. 18, 315–232.

671 Spilling, K., 2007. Dense sub-ice bloom of dinoflagellates in the Baltic Sea, potentially limited by
672 high pH. J. Plankton Res. 29, 895–901.

673 Stoecker, D.K., Buck, K.R., Putt, M., 1993. Changes in the sea-ice brine community during the
674 spring-summer transition, McMurdo Sound, Antarctica. II. Phagotrophic protists. Mar. Ecol.
675 Prog. Ser. 95, 103–113.

676 Stoecker, D.K., Johnson, M.D., de Vargas, C., Not, F., 2009. Acquired phototrophy in aquatic
677 protists. Aquat. Microb. Ecol. 57, 279–310.

678 Strom, S.L. 1993. Production of pheopigments by marine protozoa: results of laboratory
679 experiments analysed by HPLC. Deep Sea Res. I 40, 57–80.

680 Sundström, A.M., Kremp, A., Daugbjerg, N., Moestrup, Ø., Ellegaard, M., Hansen, R., Hajdu, S.,
681 2009. *Gymnodinium corollarium* sp. nov. (Dinophyceae) – a new cold-water dinoflagellate
682 responsible for cyst sedimentation events in the Baltic Sea. J. Phycol. 45, 938–952.

683 Szymczak-Zyła, M., Kowalewska, G., Louda, J.W., 2008. The influence of microorganisms on
684 chlorophyll *a* degradation in the marine environment. Limnol. Oceanogr. 53, 851–862.

685 Thaler, M., Lovejoy, C., 2012. Distribution and diversity of a protist predator *Cryothecomonas*
686 (Cercozoa) in arctic marine waters. J. Euk. Microbiol. 59, 291–299.

687 Utermöhl, H., 1958. Zur Vervollkommnung der quantitativen Phytoplankton- methodik. Mitt. Int.
688 Ver. Limnol. 9, 1–38.

689 Vørs, N., 1992. Heterotrophic amoebae, flagellates and heliozoan from the Tvärminne area, Gulf of
690 Finland, in 1988–1990. Ophelia 36, 1–109.

691 Willén, T., 1962. Studies on the phytoplankton of some lakes connected with or recently isolated
692 from the Baltic. Oikos 13, 169–199.

693 Zapata, M., Jeffrey, S.W., Wright, S.W., Rodriguez, F., Garrido, J.L., Clementson, L., 2004.
694 Photosynthetic pigments in 37 species (65 strains) of Haptophyta: implications for
695 oceanography and chemotaxonomy. Mar. Ecol. Prog. Ser. 270, 83–102.

696 Zhu, F., Massana, R., Not, F., Marie, D., Vaulot, D. 2005. Mapping of picoeucaryotes in marine
697 ecosystems with quantitative PCR of the 18S rRNA gene. FEMS Microbiol. Ecol. 52, 79–92.

698

699 **Supplementary material**

700 Supplementary table 1. Concentrations of pigments in each sample.

701 Supplementary table 2. Light microscopy (LM)-quantified biomass of taxa in each sample.

702 Supplementary file 1. Abundance of operational taxonomic units (OTUs) in each sample, their
703 taxonomy and potential nutritional mode.

704 Supplementary figure 1. Map showing the sampling locations in the Gulf of Finland, Baltic Sea.

705 Supplementary figure 2. Concentrations of pigments in an additional melting experiment.

706

707 **Figure titles and legends**

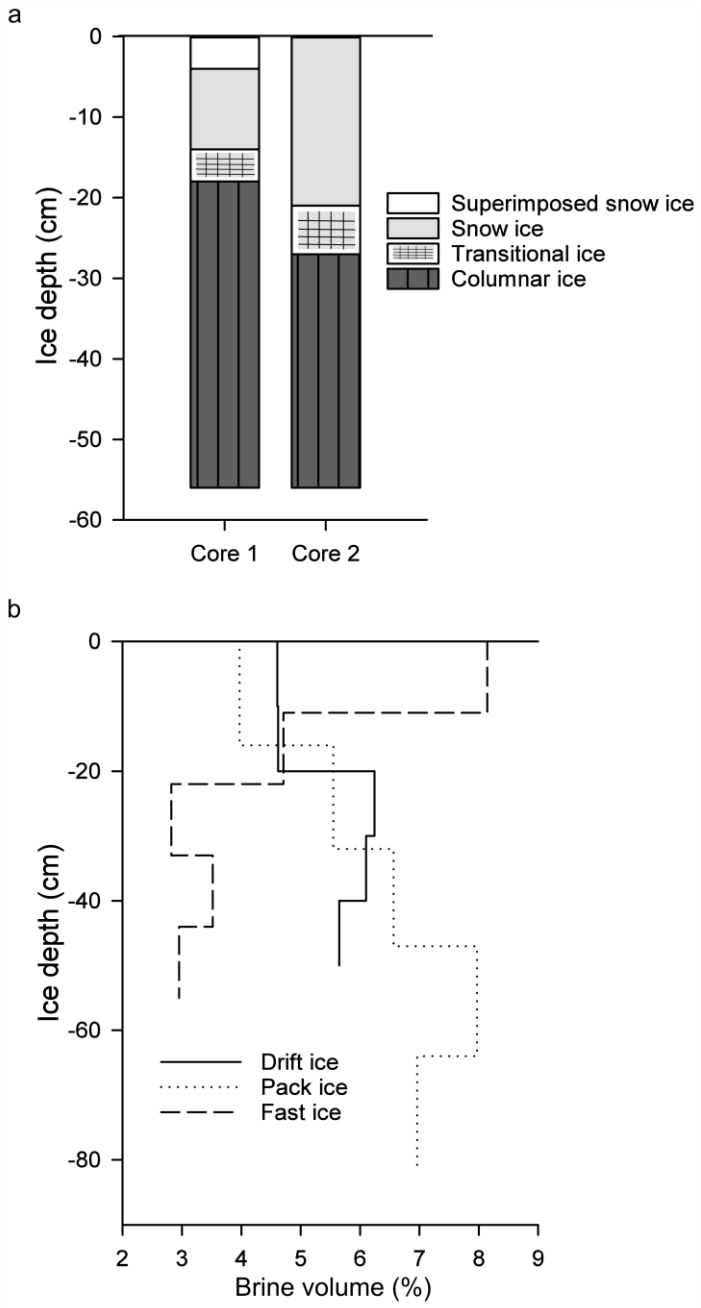

708

709 Fig. 1. Physical properties of the ice. (a) Ice structure of two cores taken from the fast-ice station.
710 (b) Estimated brine volumes at each station. We estimated the brine volumes, based on the bulk
711 salinity and average ice temperature at each section (Cox and Weeks, 1983; Leppäranta and
712 Manninen, 1988).

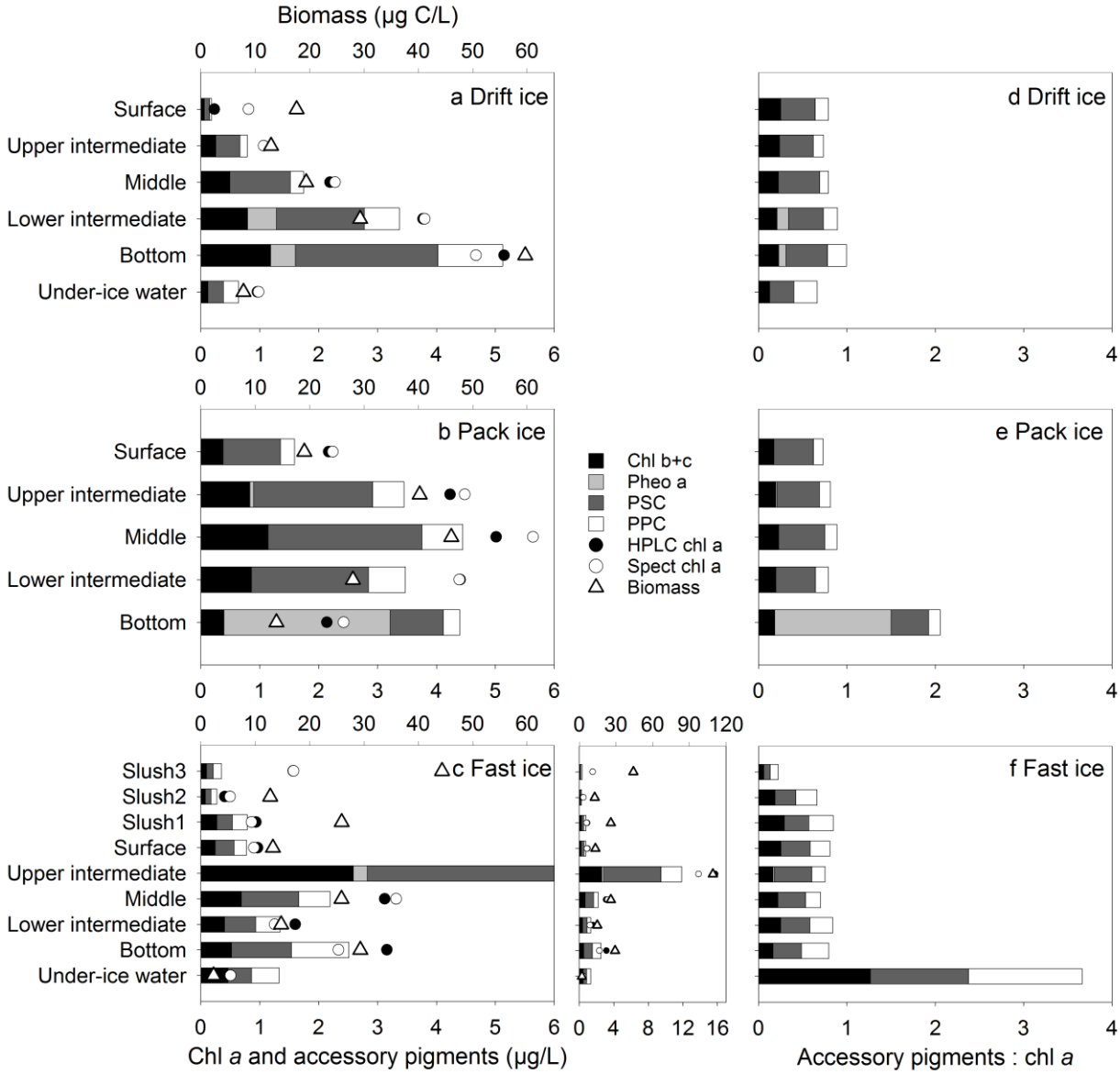

713

714 Fig. 2. Pigment composition and biomass in the samples. (a)–(c) Concentrations of pigments (µg l^{-1})
715 grouped as chlorophylls *b*+*c*, photosynthetic carotenoids (PSCs), pheophytin *a* and photoprotective
716 carotenoids (PPCs), concentrations of chlorophyll *a* (chl-*a*) measured using a spectrofluorometer
717 and HPLC, as well as total algal biomass in the (a) drift ice, (b) pack ice and (c) fast ice. The
718 additional panel illustrates high concentrations of pigments in the middle section of the fast ice. (d)–
719 (f) Ratios of total and grouped accessory pigments to chl-*a* (HPLC-measured) in the (d) drift ice, (e)

720 pack ice and (f) fast ice. The legend is the same for figures (a)–(f). See Supplementary table 1 for
721 results in detail.

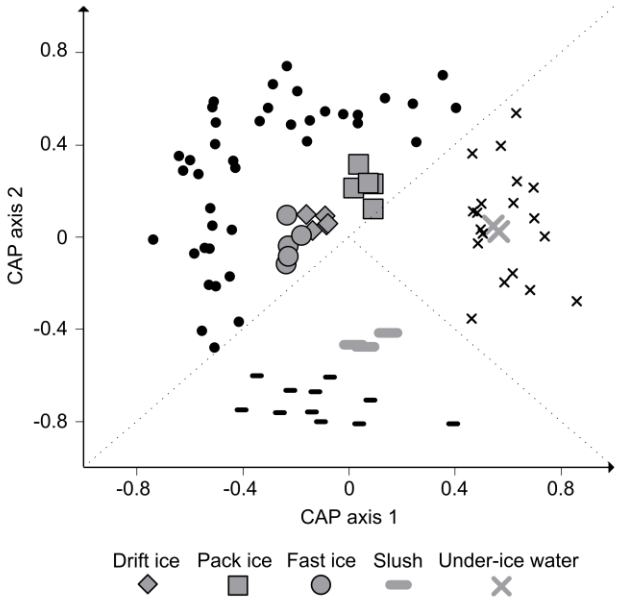

OTUs characteristic of ice

Chloroplastida:
OTU 109 *Chlamydomonas*
OTU 288 *Chlamydomonas pulsatilla*
OTU 15 *Mantoniella squamata*
Eukaryota *incertae sedis*:
OTU 167 *Falcomonas* sp.
OTU 194 *Hemiselmis* sp.
OTU 125 *Chroomonas* sp.
OTU 253 *Goniomonas*
OTU 85 *Isochrysis*
Opisthokonta:
OTU 55 Rotifera
OTU 180 *Eurytemora affinis*
Alveolata:
OTU31 *Balanion*
OTU 164 Stichotrichia
OTU 199 *Frontonia*
OTU 116 *Homalogastra setosa*
OTU 12 *Phialina*
OTU 268 *Biecheleria baltica*
OTU 64 *Heterocapsa arctica*
Rhizaria:
OTU 88 Silicofilosea
OTU 120 *Cercomonas*
OTU 8 *Ebria*
OTU 276 *Ebria*
OTU 4 Thraustochytriaceae
OTU 273 *Cryothecomonas* sp.
OTU 161 *Cryothecomonas aestivalis*
OTU 111 Protaspidae
OTU 147 *Protaspis grandis*
stramenopiles:
OTU 138 Bacillariophyceae
OTU 221 Mediophyceae
OTU 143 *Chaetoceros*
OTU 166 *Chaetoceros*
OTU 252 *Thalassiosira* sp.
OTU 217 *Skeletonema marinoi*
OTU 225 *Pauliella taeniata*
OTU 104 *Melosira arctica*
OTU 30 Chrysophyceae
OTU 134 Chrysophyceae
OTU 32 *Paraphysomonas*
OTU 133 *Paraphysomonas imperforata*
OTU 259 *Nannochloropsis limnetica*
OTU 132 MAST-1
OTU 79 Labyrinthuloides

OTUs characteristic of slush

Opisthokonta:
OTU 24 Chytridiomycota
Alveolata:
OTU 213 Alveolata
OTU 282 Spirotrichea
OTU 241 *Strombidium biarmatum*
Rhizaria:
OTU 201 Cercozoa
OTU 153 Silicofilosea
OTU 254 Silicofilosea
OTU 22 *Protaspa* sp.
OTU 234 *Mataza hastifera*
stramenopiles:
OTU 287 *Ochromonas* sp.
OTU 108 *Aureococcus* sp.

OTUs characteristic of under-ice water

Chloroplastida:
OTU 149 *Bathycoccus prasinos*
Eukaryota *incertae sedis:*
OTU 243 Cryptophyceae
OTU 44 *Teleaulax amphioxeia*
OTU 219 *Chrysochromulina*
OTU 200 *Telonema subtilis*
OTU 216 Picozoa
Opisthokonta:
OTU 278 Fungi
OTU 227 *Rhodotorula mucilaginosa*
OTU 101 *Diaphanoeca*
Alveolata:
OTU 196 Ciliophora
OTU 71 Choreotrichia
OTU 156 Choreotrichia
OTU 270 *Cryptocaryon*
OTU 23 Haptoria
OTU 42 Mesodiniidae
OTU 240 Mesodiniidae
OTU 95 *Mesodinium rubrum*
OTU 146 Oligotrichia
OTU 249 *Strombidium chlorophilum*
OTU 84 *Heterocapsa*
OTU 170 Gymnodiniaceae
OTU 197 Karlodinium
OTU 281 Gyrodinium
OTU 38 Syndiniales
OTU 233 Syndiniales
OTU 48 Perkinsidae
Rhizaria:
OTU 165 Cercozoa
OTU 49 Thecofilosea
stramenopiles:
OTU 217 *Thalassiosira*
OTU 35 Chrysophyceae
OTU 205 Chromulinales
OTU 179 *Ochromonas*
OTU 103 Bolidomonas
OTU 115 Dictyochophyceae
OTU 264 Pedinellales

722

723 Fig. 3. Discriminant analysis, using the abundance of 97% OTUs as variables and sample type as a
724 grouping variable. Analysis was based on Jaccard dissimilarity and eight first principal coordinates
725 (83.79 % of the variability explained). Here, only the first two canonical axes are illustrated (four in
726 total). The large grey symbols represent the samples, and the small black symbols are the individual
727 OTUs responsible for the multivariate pattern (strong to moderate correlation with either both or
728 one of the canonical axes, n = 86). These OTUs are listed. Phototrophic taxa are in bold.

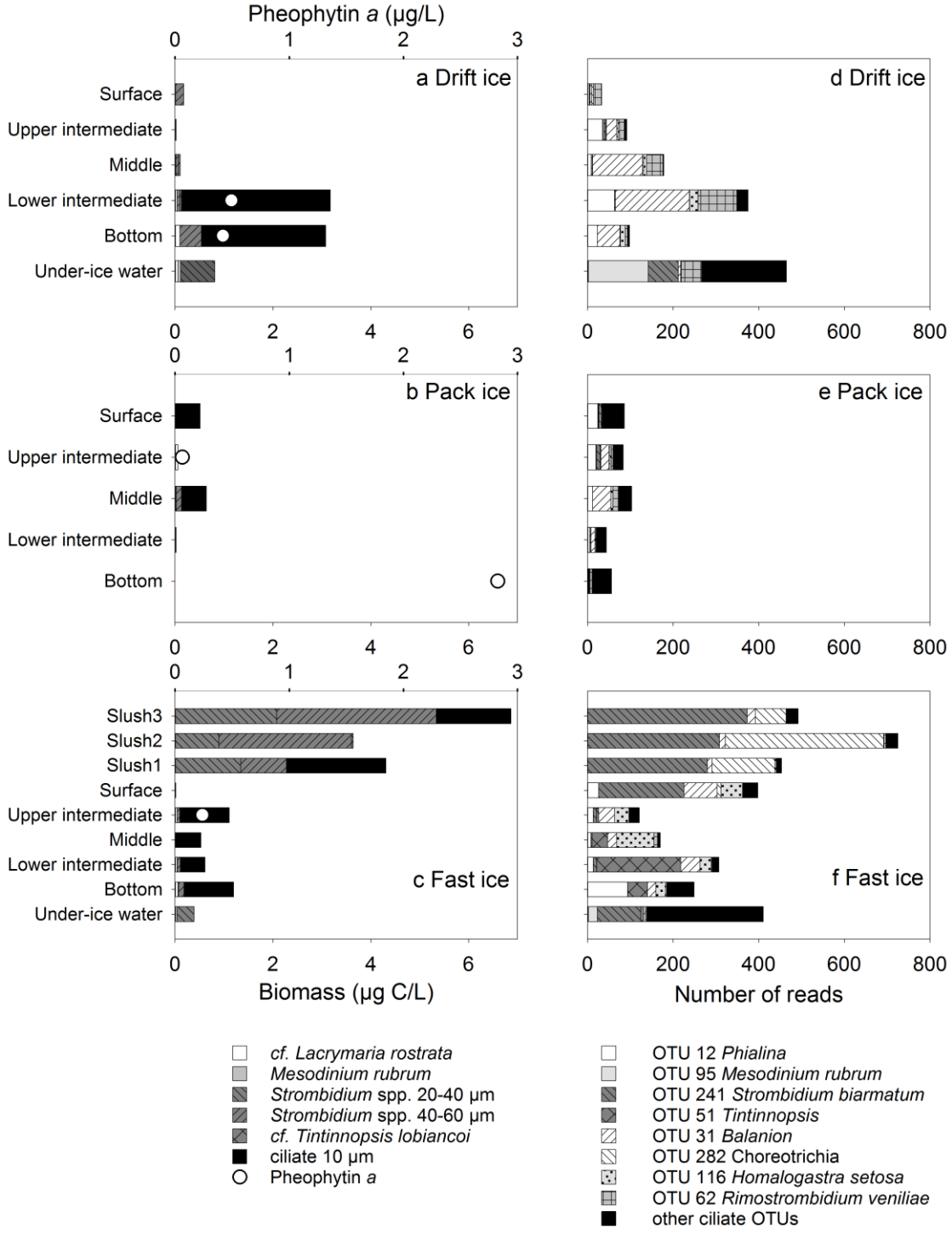

729

730 Fig. 4. Biomass of light microscopy (LM)-enumerated algae (µg C l^{-1}) in the (a) drift ice, (b) pack
731 ice and (c) fast ice. The additional panel illustrates high biomass in the middle section of the fast
732 ice. See Supplementary table 2 for results in detail.

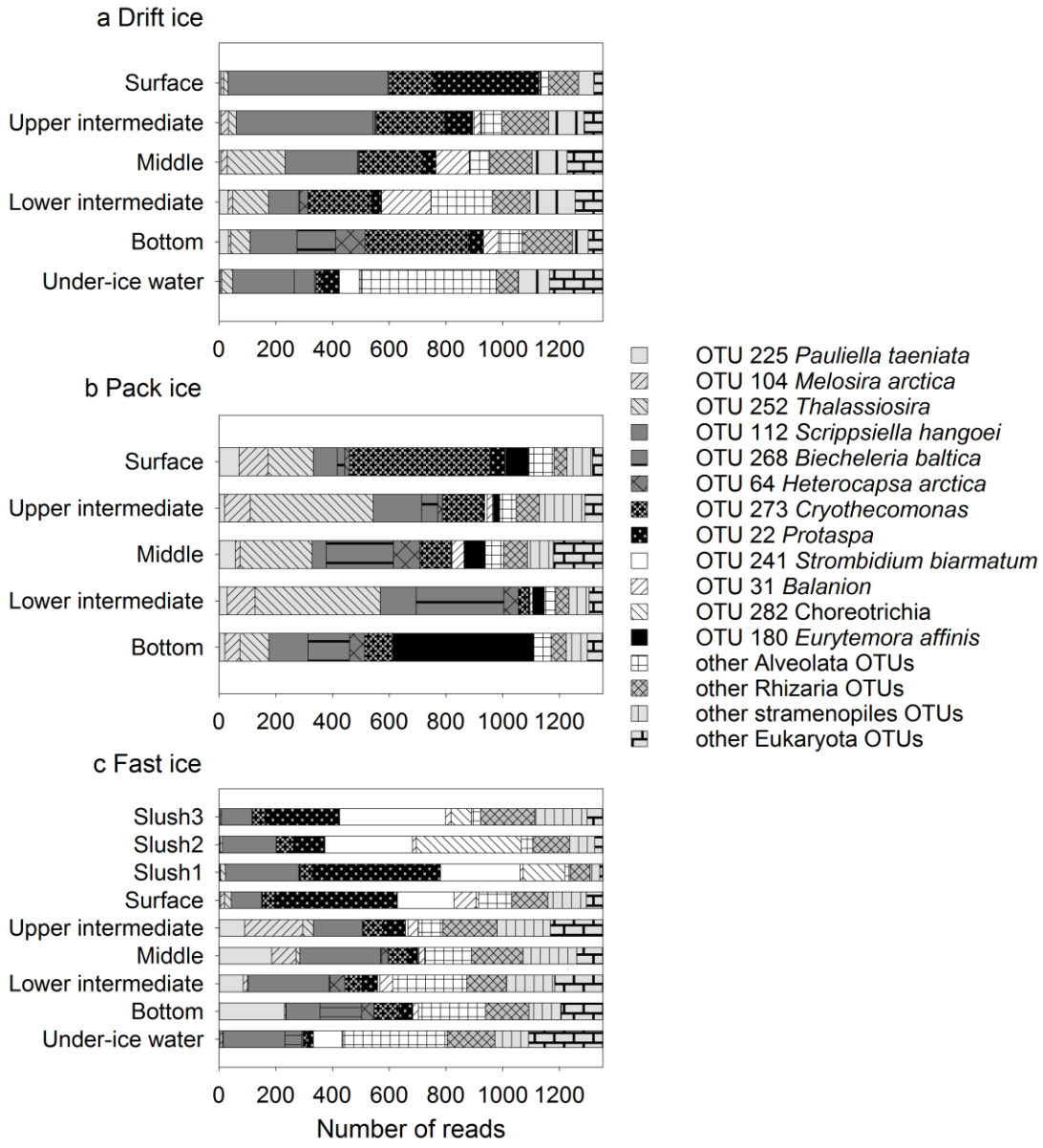

733

734 Fig. 5. Read abundance of OTUs in the (a) drift ice, (b) pack ice and (c) fast ice. Twelve most

735 abundant OTUs overall named after the closest known match.

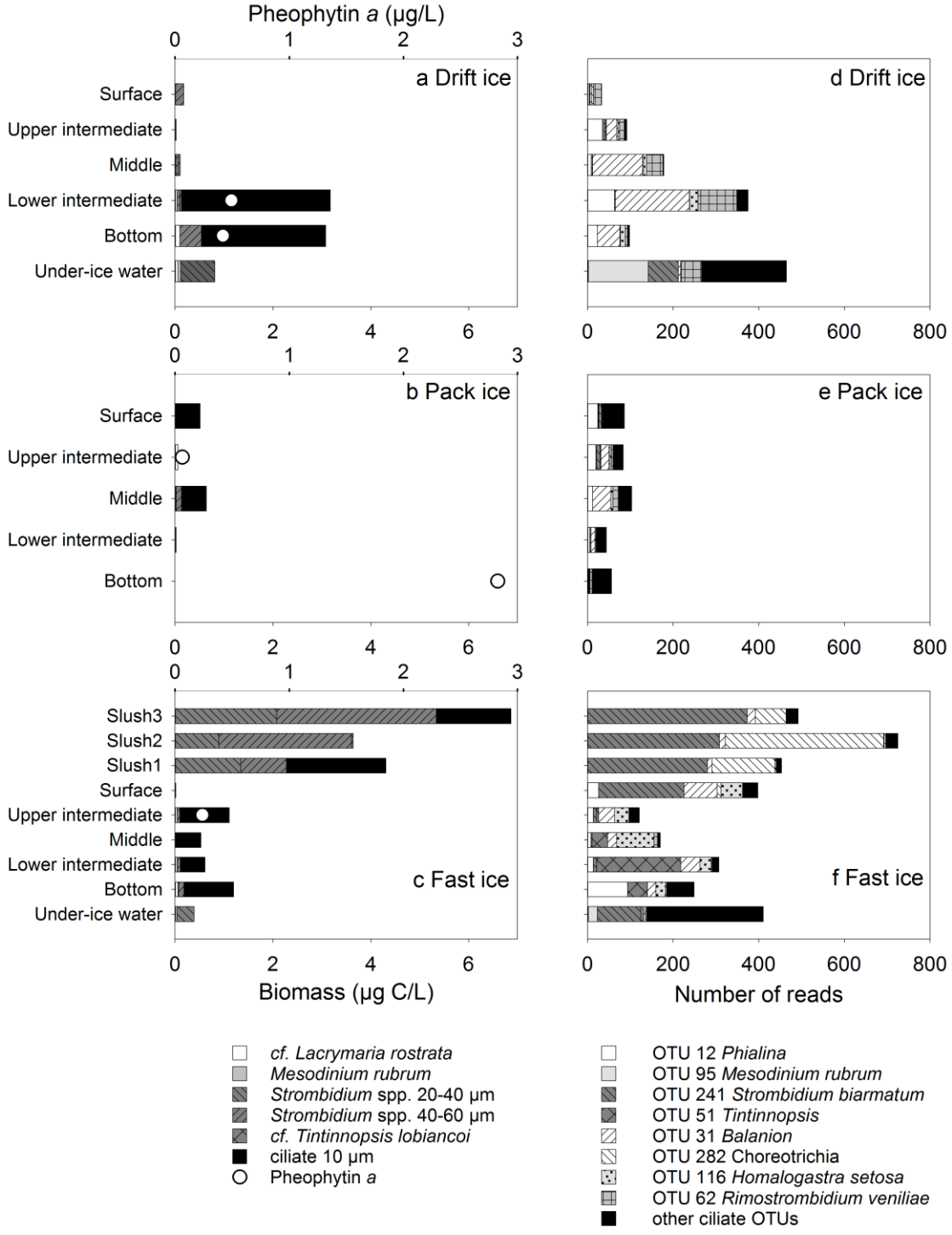

Fig. 6. Biomass of LM-enumerated ciliates and concentration of pheophytin *a* in the (a) drift ice, (b) pack ice and (c) fast ice, as well as read abundance of eight most abundant ciliate OTUs in the (d) drift ice, (e) pack ice and (f) fast ice.